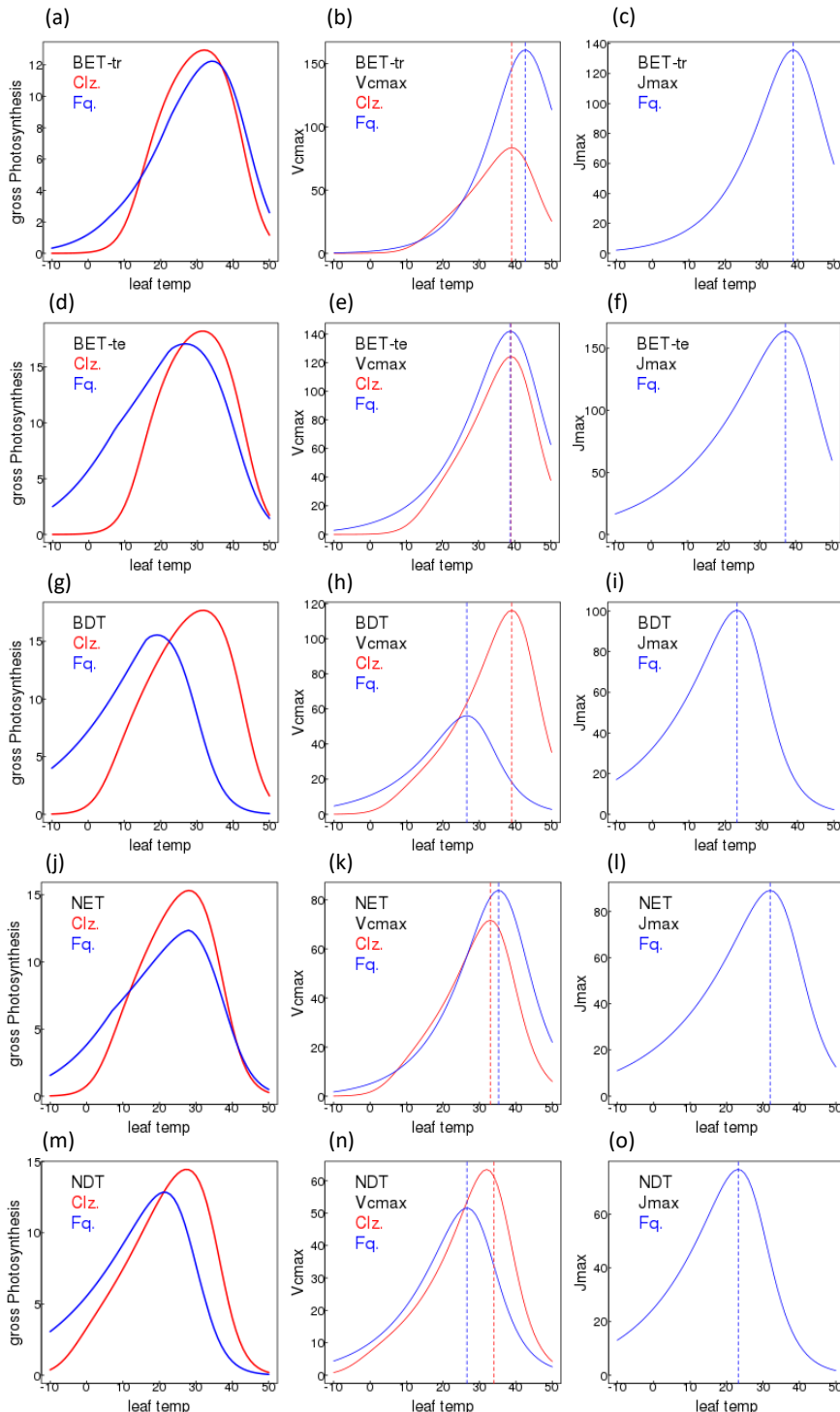


Supplementary Information

Figure S1. Simple leaf-level model of gross photosynthesis to show the temperature dependency of gross photosynthesis, V_{cmax} and J_{max} for Collatz (Clz. red) and Farquhar (Fq. blue) with PFT specific parameters (Table 1 and 2) for all 9 JULES PFTs. The dotted vertical lines show the T_{opt} for V_{cmax} and J_{max} .

These temperature response curves were produced using simplified Collatz and Farquhar leaf-level models of gross photosynthesis where all environmental variables were fixed (light (300 W m⁻² PAR), CO₂ concentration (31 Pa), without water stress), apart from air temperature which was allowed to change in the range of -10 to 50°C. Each PFT was parameterised with PFT specific values from Tables 1 and 2. The resulting temperature dependencies are shown below, and are helpful in interpreting the results of the large scale simulations.



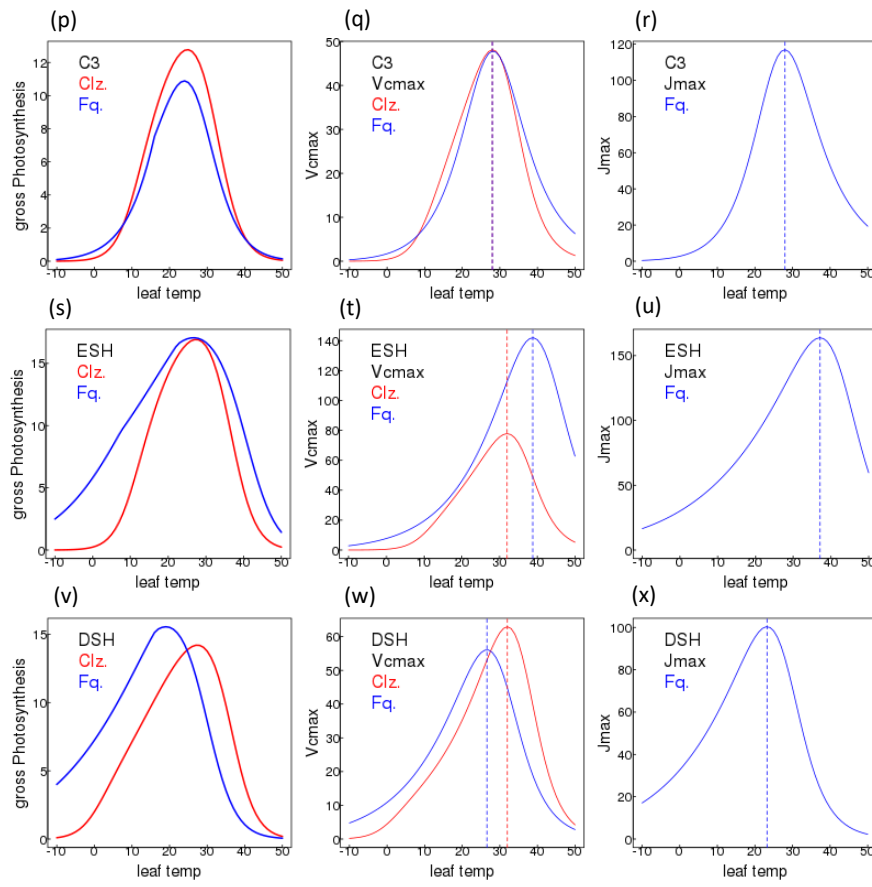


Figure S2. Location of eddy covariance Flux tower sites used in site-level evaluation. 14 sites were from the Fluxnet tower network (<https://fluxnet.org/data/fluxnet2015-dataset/>), and three were from the LBA-ECO Flux tower network (https://daac.ornl.gov/LBA/guides/CD32_Brazil_Flux_Network.html) (Restrepo-Coupe et al., 2013).

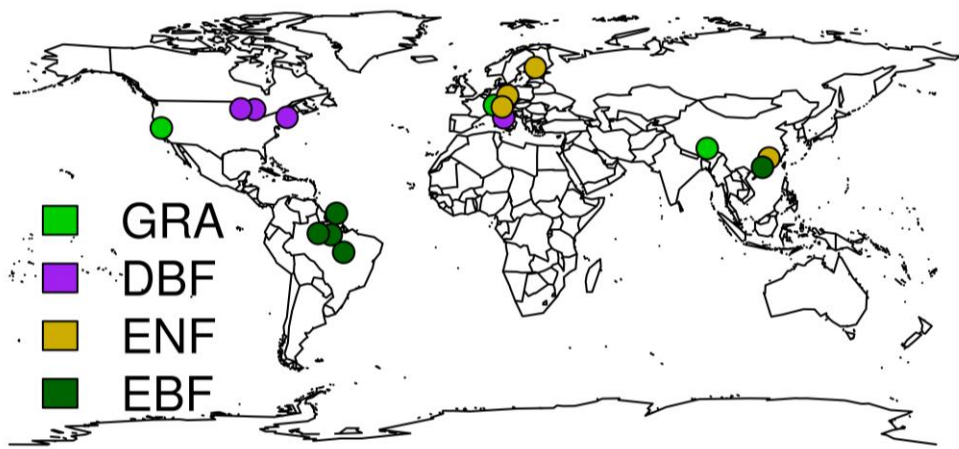


Table S1. Information on Fluxnext 2015 (14 sites) and Brasilflux sites* (3 sites) used for site-level model evaluation. IGBP vegetation types correspond to Evergreen Broadleaved forest & Evergreen Needle leaved Forest (EBF & ENF), Deciduous Broadleaved forest (DBF) and C₃ grasses (GRA). The fractional coverage of each vegetation type as represented by the JULES plant functional types is also given: broad leaved deciduous trees (BDT), evergreen needle leaved trees (NET), C₃ grasses (C3) and broad leaved evergreen tropical (BET-tr).

Site	Country	Latitude	Longitude	IGBP	JULES fracs
CN_Dan	China	30.50	91.07	GRA	100% C3
AT_Neu	Austria	47.12	11.32	GRA	100% C3
CH_Cha	Switzerland	47.21	8.41	GRA	100% C3
US_Var	USA	38.41	-120.95	GRA	100% C3
US_UMB	USA	45.56	-84.71	DBF	100% BDT
US_Ha1	USA	42.54	-72.17	DBF	100% BDT
IT_CA1	Italy	42.38	12.03	DBF	100% BDT
US_WCr	USA	45.81	-90.08	DBF	100% BDT
FI_Hyy	Finland	61.85	24.30	ENF	100% NET
DE_Tha	Germany	50.96	13.57	ENF	100% NET
CN_Qia	China	26.74	115.06	ENF	100% NET
IT_Ren	Italy	46.59	11.43	ENF	100% NET
GF_Guy	French Guiana	5.28	-52.92	EBF	100 % BET-tr
CN_Din	China	23.17	112.54	EBF	100 % BET-tr
LBA_K83*	Brazil	-3.02	-54.97	EBF	100 % BET-tr
LBA_K34*	Brazil	-2.50	-60.00	EBF	100 % BET-tr
LBA_BAN*	Brazil	-9.82	-50.16	EBF	100 % BET-tr

Figure S3. Fractional cover of each JULES land cover type.

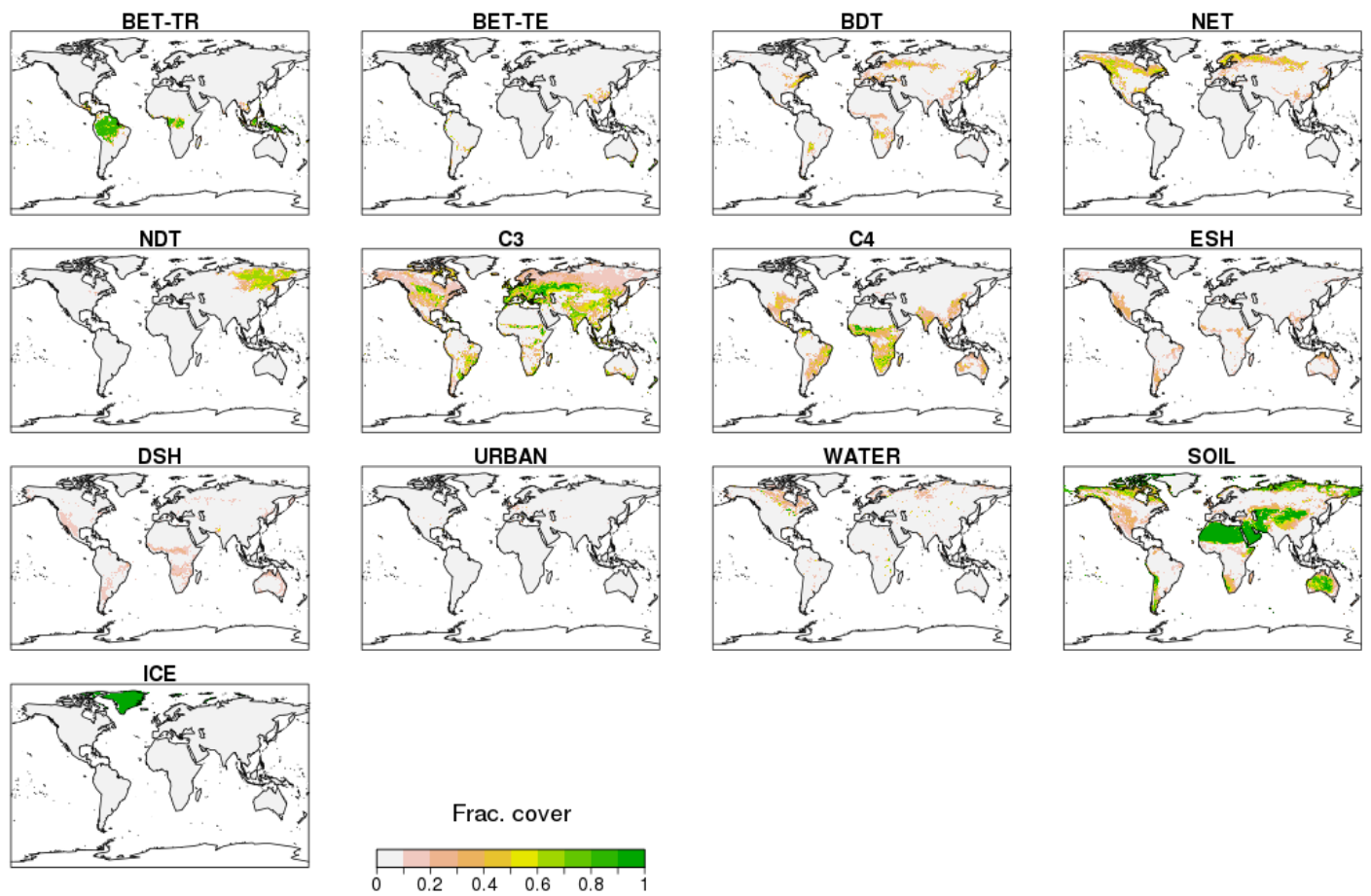


Figure S4. The mean air temperature ($^{\circ}\text{C}$) and precipitation (mm day^{-1}) change by region over the study period (1960 to 2050), and the atmospheric CO₂ concentration (ppm).

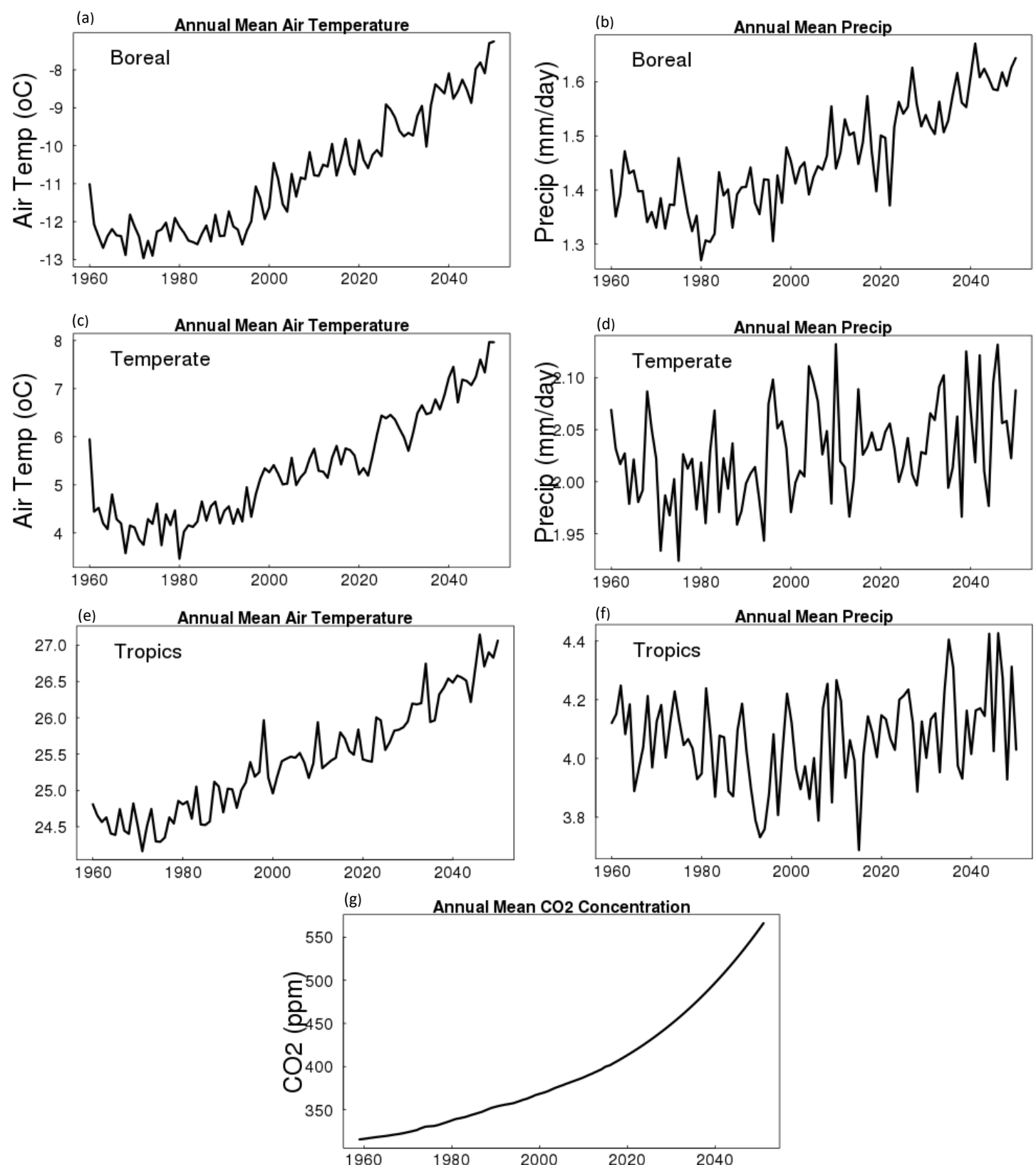


Figure S5. Sensitivity of simulated intercellular CO₂ concentration (ci) to leaf-level specific humidity deficit (DQC) for the Jacobs and Medlyn g_s models at LBA-K34 (left-hand panel of plots) and FI-Hyy (right-hand panel of plots) FLUXNET sites.

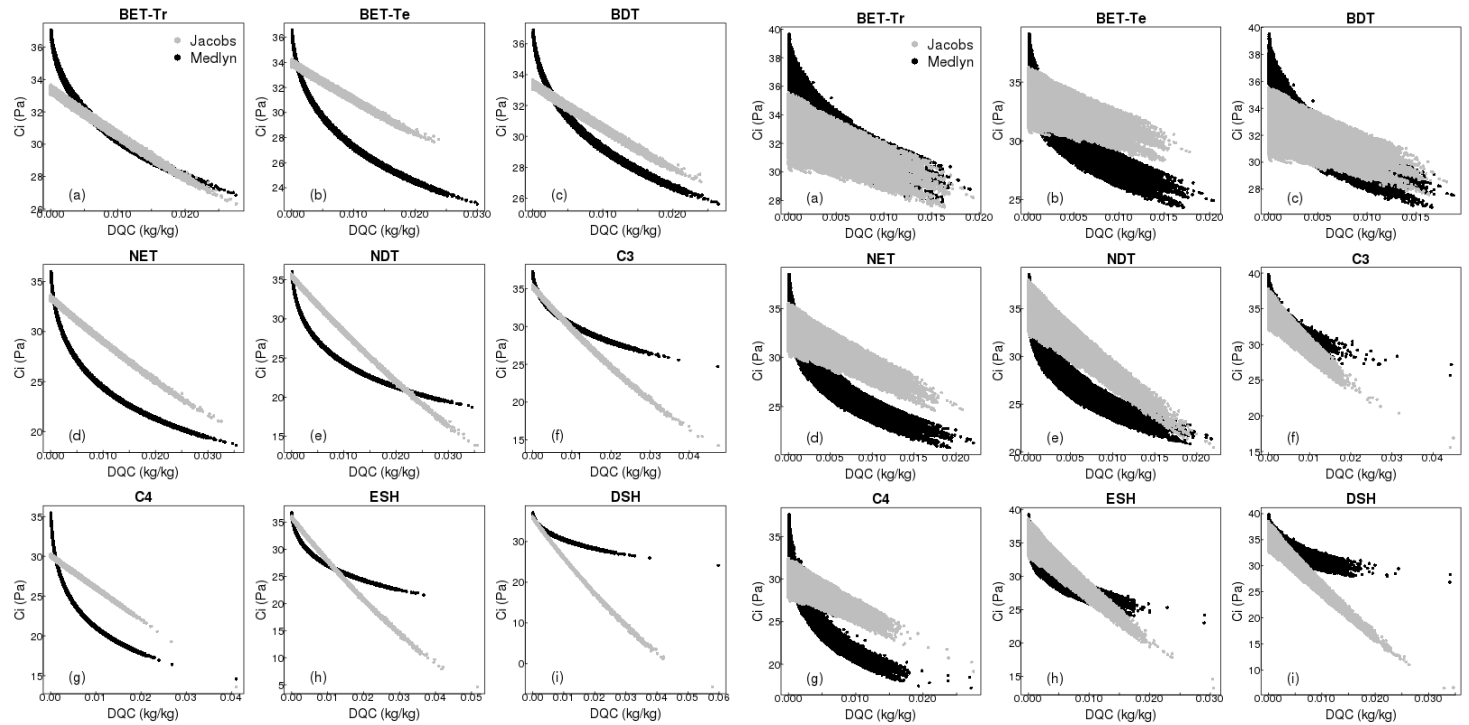


Figure S6. Differences between JULES modelled GPP, latent (LE) and sensible heat (H) for the different JULES model configurations in December-January-February (DJF). For each variable the mean over the period 2002 to 2012 is used.

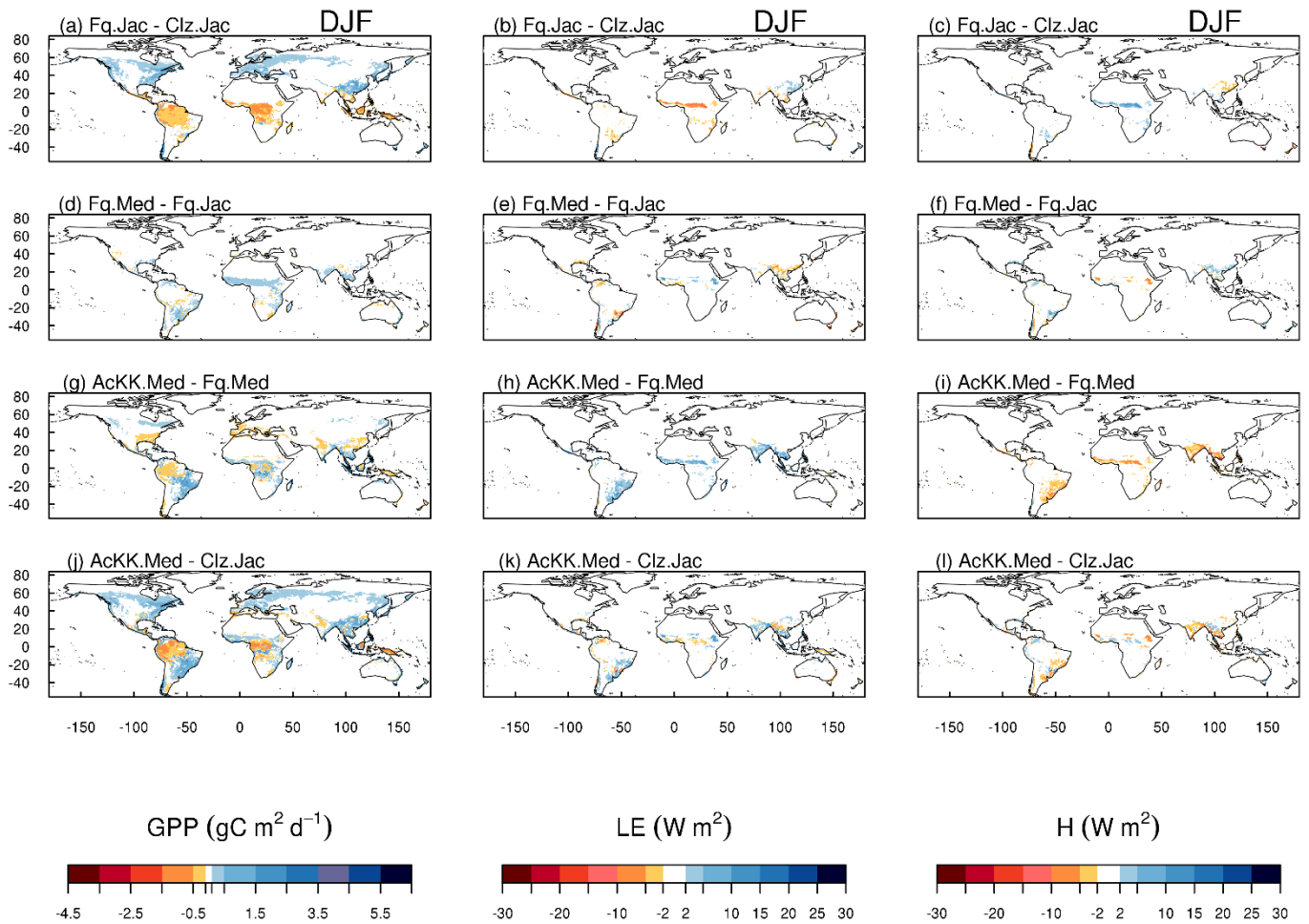


Table S2. Seasonal mean (and annual mean) global GPP (Pg C) of each JULES model configuration and global GPP products FluxCom and MOD17.

	GPP Pg C season ⁻¹				Pg C yr ⁻¹
	JJA	MAM	SON	DJF	Annual
FluxCom	44.7	32.5	29.4	25.7	132.3
MOD17	39.0	26.8	25.5	20.4	111.7
Clz.Jac	42.2	28.8	34.5	24.8	130.3
Fq.Jac	41.7	29.1	34.4	25.0	130.2
Fq.Med	42.0	29.5	34.5	25.3	131.3
AcKK.Med	43.1	30.9	35.4	26.3	135.7

Table S3. Seasonal mean ET of each JULES model configuration and global ET products from FluxCom and GLEAM.

	ET mm season ⁻¹				mm yr ⁻¹
	JJA	MAM	SON	DJF	Annual
FluxCom	203.32	148.12	114.66	90.90	557.00
Gleam	199.64	143.52	113.75	92.70	549.61
Clz.Jac	194.12	126.04	153.79	100.80	574.75
Fq.Jac	192.28	125.12	153.79	99.90	571.09
Fq.Med	190.44	125.12	151.97	99.00	566.53
AcKK.Med	192.28	126.04	152.88	100.80	572.00

Table S4. Latitude mean RMSE by region and season for GPP ($\text{gC m}^2 \text{ d}^{-1}$) simulated by each model configuration compared to the FluxCom global GPP product.

Tropics: -20S TO 20N		RMSE (GPP $\text{gC m}^2 \text{ d}^{-1}$)			
		JJA	MAM	SON	DJF
Clz.Jac		1.45	1.28	1.08	1.31
Fq.Jac		1.33	1.10	0.99	1.25
Fq.Med		1.40	1.14	1.00	1.30
AcKK.Med		1.38	1.38	1.27	1.32
Sub-tropics: 20N to 30N					
Clz.Jac		0.94	0.41	1.27	1.03
Fq.Jac		0.97	0.32	1.18	1.19
Fq.Med		1.00	0.26	1.14	1.23
AcKK.Med		0.61	0.32	1.92	1.22
Sub-tropics: -20S to -30S					
Clz.Jac		0.23	0.23	0.58	1.35
Fq.Jac		0.30	0.22	0.52	1.35
Fq.Med		0.34	0.29	0.46	1.29
AcKK.Med		0.30	0.46	0.49	1.28
Temperate N: 30N to 60N					
Clz.Jac		0.61	0.89	1.24	0.11
Fq.Jac		0.72	0.70	1.34	0.26
Fq.Med		0.72	0.70	1.34	0.26
AcKK.Med		0.66	0.66	1.28	0.25
Temperate S: -30S to -60S					
Clz.Jac		0.24	0.60	0.93	0.62
Fq.Jac		0.19	0.91	0.47	0.66
Fq.Med		0.18	0.87	0.46	0.62
AcKK.Med		0.19	0.81	0.51	0.57
Boreal: 60N+					
Clz.Jac		0.95	0.25	0.86	0.13
Fq.Jac		0.94	0.15	0.98	0.15
Fq.Med		0.93	0.15	1.00	0.15
AcKK.Med		0.95	0.06	0.95	0.16

Table S5. Latitude mean RMSE by region and season for GPP ($\text{gC m}^2 \text{ d}^{-1}$) simulated by each model configuration compared to the MOD17 global GPP product.

Tropics: -20S TO 20N		RMSE (GPP $\text{gC m}^2 \text{ d}^{-1}$)			
		JJA	MAM	SON	DJF
Clz.Jac		0.99	1.08	1.35	1.09
Fq.Jac		0.80	0.82	1.20	0.90
Fq.Med		0.86	0.88	1.23	0.97
AcKK.Med		0.99	1.15	1.51	1.12
Sub-tropics: 20N to 30N					
Clz.Jac		0.34	0.59	1.26	0.45
Fq.Jac		0.29	0.50	1.17	0.68
Fq.Med		0.26	0.55	1.12	0.71
AcKK.Med		0.52	0.51	1.90	0.69
Sub-tropics: -20S to -30S					
Clz.Jac		0.50	0.30	0.67	0.47
Fq.Jac		0.39	0.27	0.60	0.47
Fq.Med		0.36	0.25	0.55	0.41
AcKK.Med		0.41	0.33	0.58	0.30
Temperate N: 30N to 60N					
Clz.Jac		0.49	0.77	0.91	0.07
Fq.Jac		0.50	0.57	1.02	0.22
Fq.Med		0.52	0.57	1.03	0.22
AcKK.Med		0.54	0.54	0.96	0.21
Temperate S: -30S to -60S					
Clz.Jac		0.41	0.58	1.20	0.73
Fq.Jac		0.35	0.83	0.75	0.60
Fq.Med		0.34	0.78	0.74	0.54
AcKK.Med		0.39	0.73	0.79	0.52
Boreal: 60N+					
Clz.Jac		1.32	0.22	0.71	0.01
Fq.Jac		1.27	0.12	0.83	0.03
Fq.Med		1.27	0.12	0.84	0.03
AcKK.Med		1.26	0.03	0.80	0.04

Table S6. Latitude mean RMSE by region and season for ET (mm d⁻¹) simulated by each model configuration compared to the FluxCom global ET product.

Tropics: -20S TO 20N		RMSE (ET mm d ⁻¹)			
		JJA	MAM	SON	DJF
Clz.Jac		0.37	0.58	0.31	0.25
Fq.Jac		0.36	0.58	0.32	0.22
Fq.Med		0.38	0.57	0.29	0.23
AcKK.Med		0.40	0.59	0.31	0.26
Sub-tropics: 20N to 30N					
Clz.Jac		0.34	0.45	0.51	0.18
Fq.Jac		0.36	0.46	0.48	0.17
Fq.Med		0.41	0.47	0.43	0.15
AcKK.Med		0.37	0.48	0.54	0.19
Sub-tropics: -20S to -30S					
Clz.Jac		0.14	0.60	0.38	0.28
Fq.Jac		0.15	0.59	0.38	0.30
Fq.Med		0.14	0.57	0.37	0.31
AcKK.Med		0.13	0.61	0.38	0.27
Temperate N: 30N to 60N					
Clz.Jac		0.39	0.51	0.79	0.19
Fq.Jac		0.43	0.49	0.79	0.20
Fq.Med		0.41	0.50	0.76	0.20
AcKK.Med		0.37	0.50	0.77	0.20
Temperate S: -30S to -60S					
Clz.Jac		0.23	0.66	0.35	0.35
Fq.Jac		0.24	0.68	0.32	0.36
Fq.Med		0.24	0.67	0.33	0.37
AcKK.Med		0.24	0.67	0.34	0.36
Boreal: 60N+					
Clz.Jac		0.38	0.39	0.63	0.13
Fq.Jac		0.38	0.39	0.63	0.14
Fq.Med		0.38	0.39	0.62	0.14
AcKK.Med		0.37	0.38	0.61	0.14

Table S7. Latitude mean RMSE by region and season for ET (mm d^{-1}) simulated by each model configuration compared to the GLEAM global ET product.

Tropics: -20S TO 20N		RMSE (ET mm d^{-1})			
		JJA	MAM	SON	DJF
Clz.Jac		0.29	0.50	0.39	0.35
Fq.Jac		0.28	0.50	0.40	0.34
Fq.Med		0.29	0.49	0.37	0.35
AcKK.Med		0.31	0.52	0.40	0.37
Sub-tropics: 20N to 30N					
Clz.Jac		0.22	0.23	0.64	0.18
Fq.Jac		0.24	0.24	0.61	0.18
Fq.Med		0.29	0.26	0.56	0.16
AcKK.Med		0.25	0.26	0.66	0.19
Sub-tropics: -20S to -30S					
Clz.Jac		0.21	0.80	0.22	0.14
Fq.Jac		0.23	0.79	0.21	0.13
Fq.Med		0.21	0.76	0.22	0.12
AcKK.Med		0.20	0.80	0.23	0.13
Temperate N: 30N to 60N					
Clz.Jac		0.08	0.46	0.83	0.22
Fq.Jac		0.10	0.44	0.82	0.22
Fq.Med		0.12	0.45	0.80	0.22
AcKK.Med		0.11	0.45	0.81	0.21
Temperate S: -30S to -60S					
Clz.Jac		0.33	0.72	0.46	0.25
Fq.Jac		0.34	0.74	0.42	0.21
Fq.Med		0.34	0.74	0.43	0.23
AcKK.Med		0.34	0.73	0.44	0.23
Boreal: 60N+					
Clz.Jac		0.38	0.29	0.59	0.06
Fq.Jac		0.37	0.29	0.60	0.06
Fq.Med		0.41	0.29	0.58	0.06
AcKK.Med		0.41	0.28	0.57	0.06

Figure S7. Colours indicate the JULES model configuration that gives the lowest RMSE compared to either the a) FluxCom or b) MOD17 global GPP ($\text{gC m}^2 \text{ day}^{-1}$), or c) FluxCom or d) GLEAM global ET (mm day^{-1}) products for DJF over the period 2002 to 2012. Actual RMSE values shown in Fig. S10 and Fig. S11.

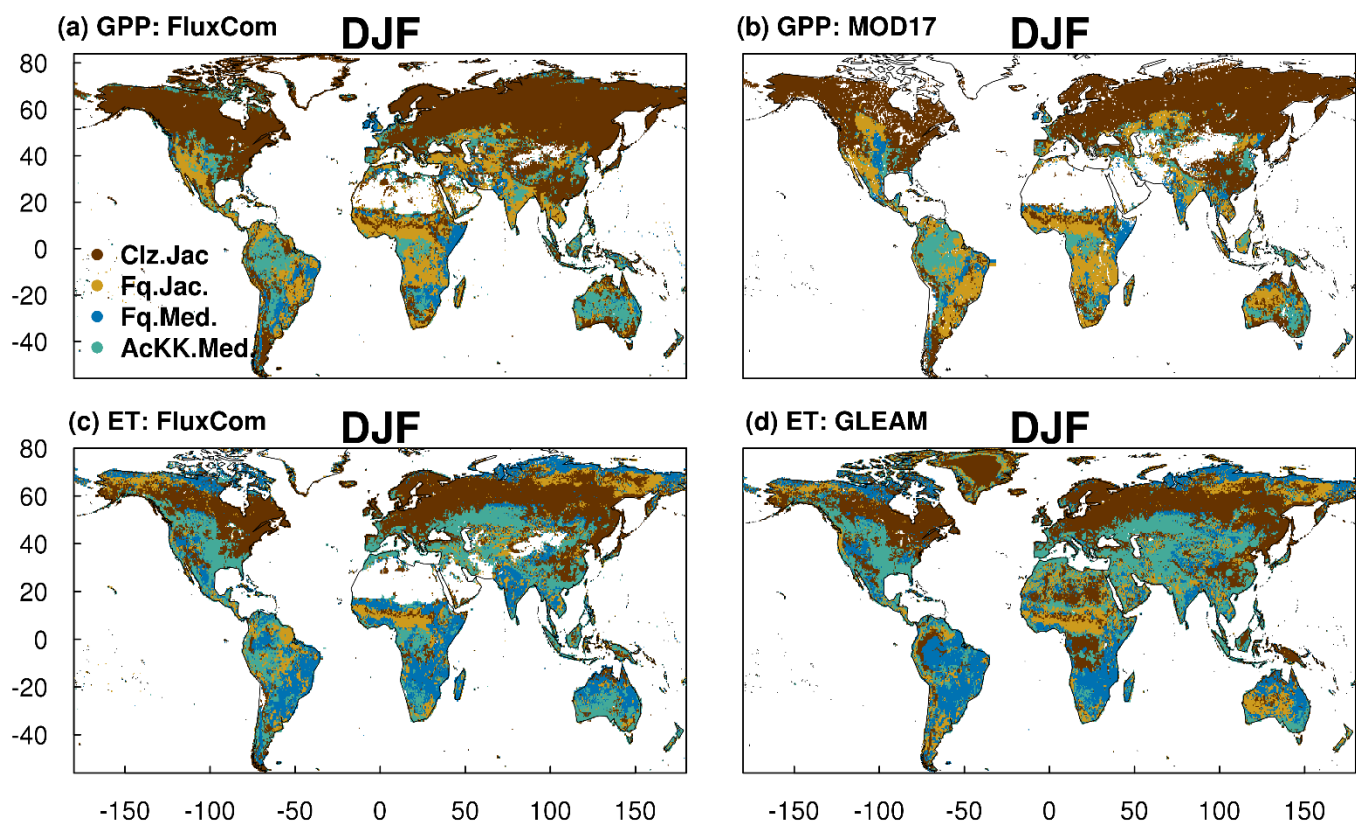


Figure S8. RMSE of GPP ($\text{gC m}^2 \text{ day}^{-1}$) in JJA for each JULES model configuration compared to either FluxCom or MOD17 global GPP products.

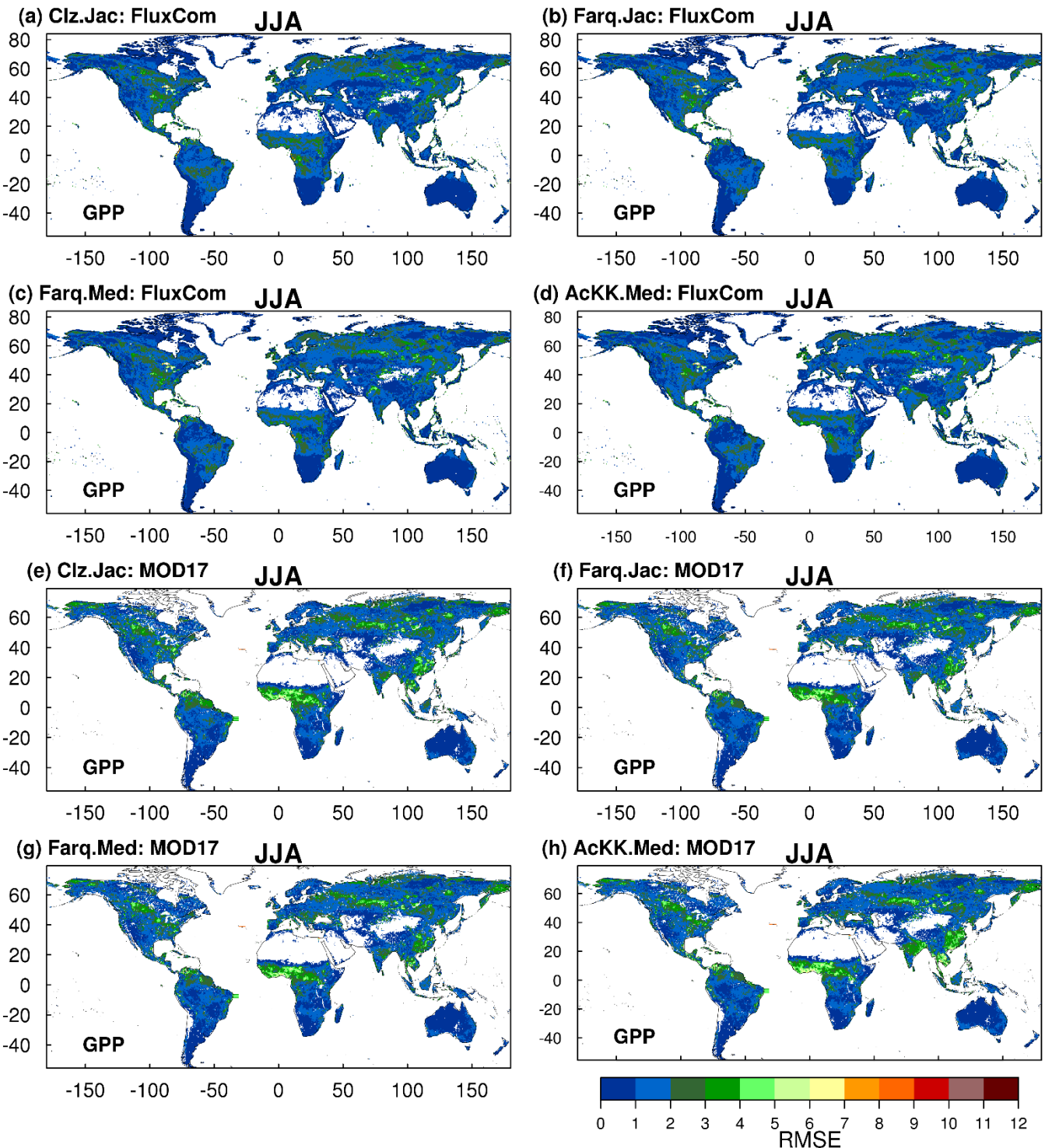


Figure S9. RMSE of ET (mm day^{-1}) in JJA for each JULES model configuration compared to either FluxCom or GLEAM global ET products.

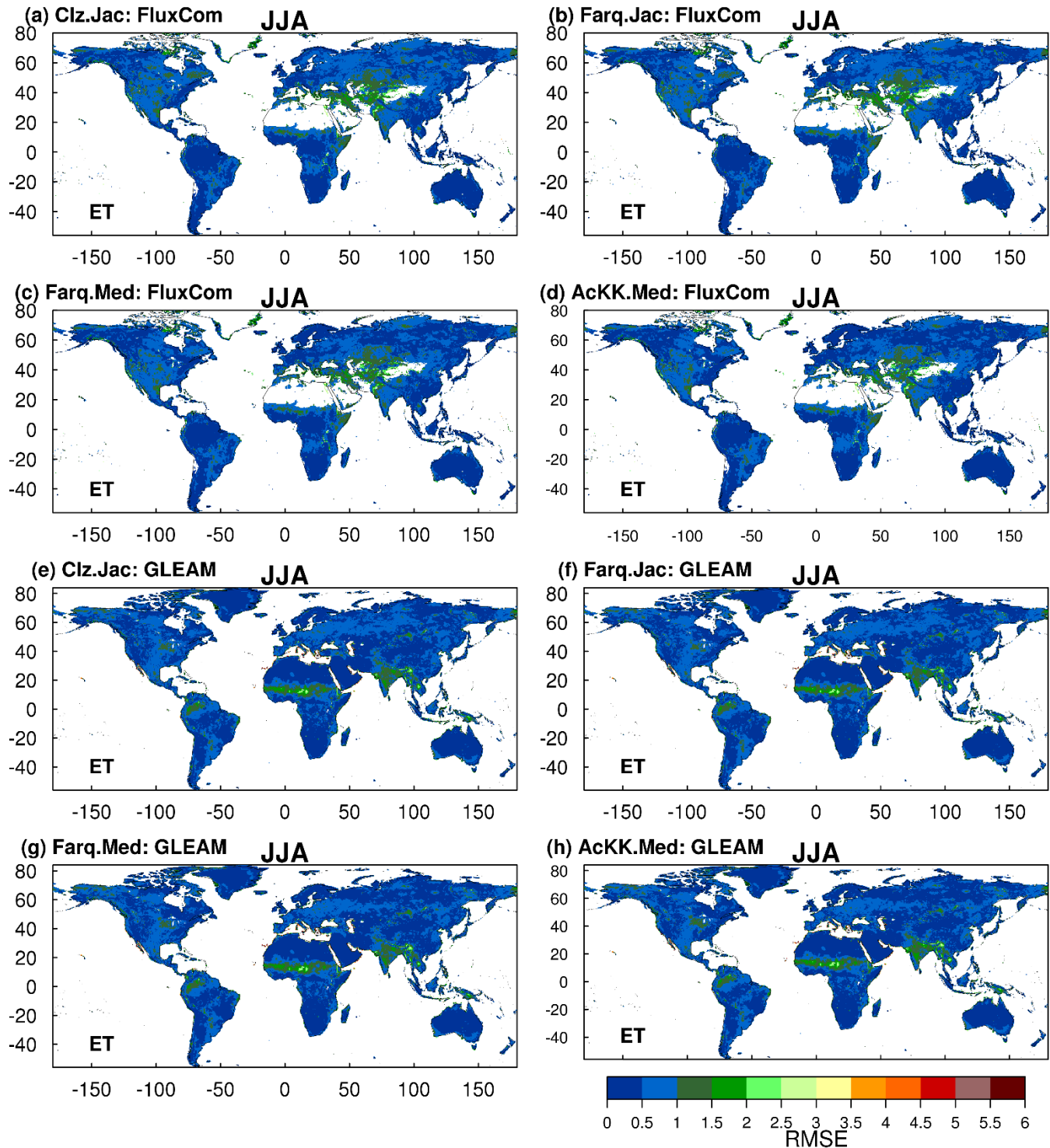


Figure S10. RMSE of GPP ($\text{gC m}^2 \text{ day}^{-1}$) in DJF for each JULES model configuration compared to either FluxCom or MOD17 global GPP products.

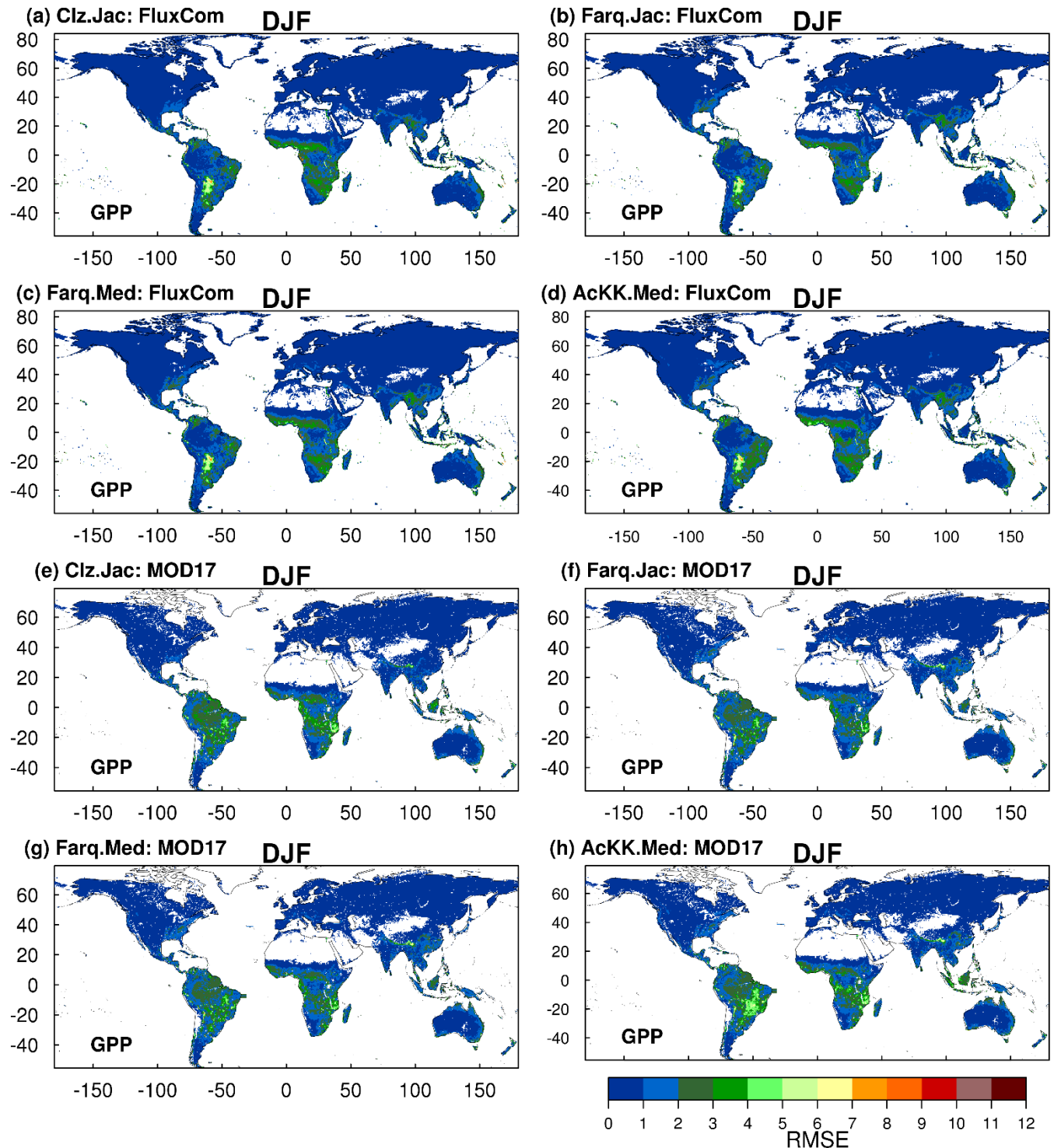


Figure S11. RMSE of ET (mm day^{-1}) in DJF for each JULES model configuration compared to either FluxCom or GLEAM global GPP products.

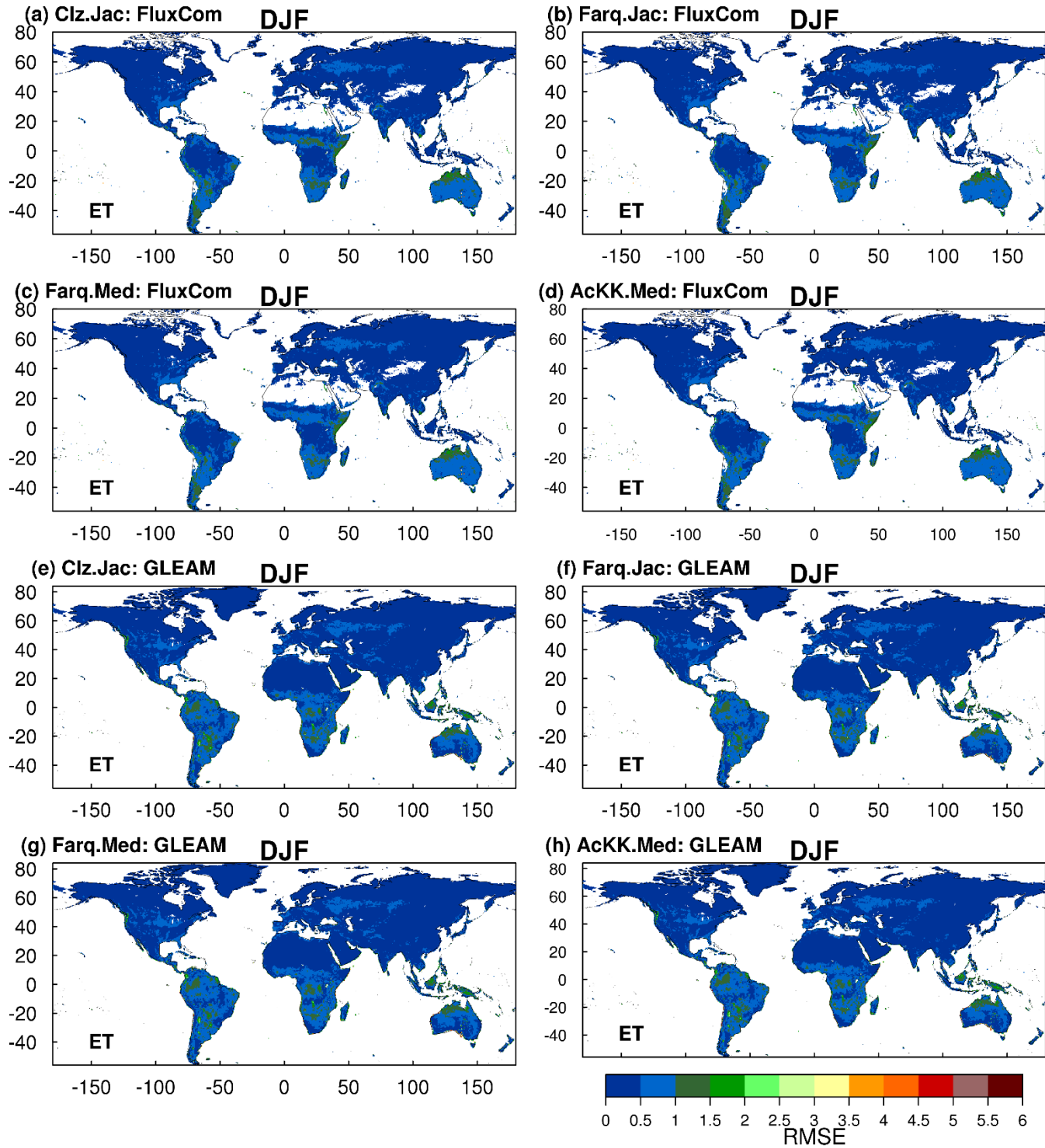
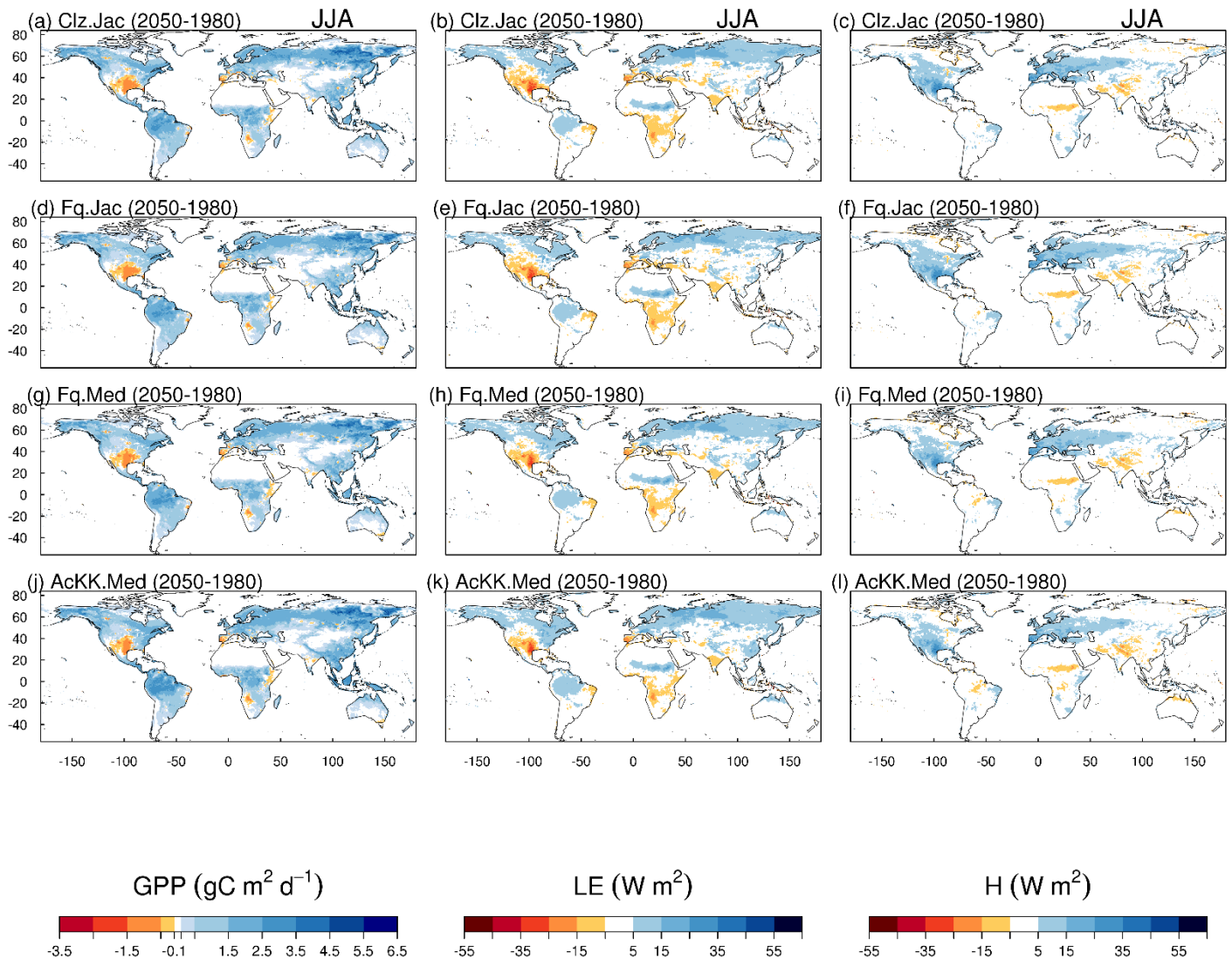


Figure S12. Change in simulated GPP ($\text{g C m}^{-2} \text{ day}^{-1}$), LE (W m^{-2}) and H (W m^{-2}) over the study period (1980 to 2050) with each model configuration.



Restrepo-Coupe, N., da Rocha, H. R., Hutyra, L. R., da Araujo, A. C., Borma, L. S., Christoffersen, B., Cabral, O. M. R., de Camargo, P. B., Cardoso, F. L., da Costa, A. C. L., Fitzjarrald, D. R., Goulden, M. L., Kruijt, B., Maia, J. M. F., Malhi, Y. S., Manzi, A. O., Miller, S. D., Nobre, A. D., von Randow, C., Sá, L. D. A., Sakai, R. K., Tota, J., Wofsy, S. C., Zanchi, F. B., and Saleska, S. R.: What drives the seasonality of photosynthesis across the Amazon basin? A cross-site analysis of eddy flux tower measurements from the Brasil flux network, Agricultural and Forest Meteorology, 182-183, 128-144, <https://doi.org/10.1016/j.agrformet.2013.04.031>, 2013.